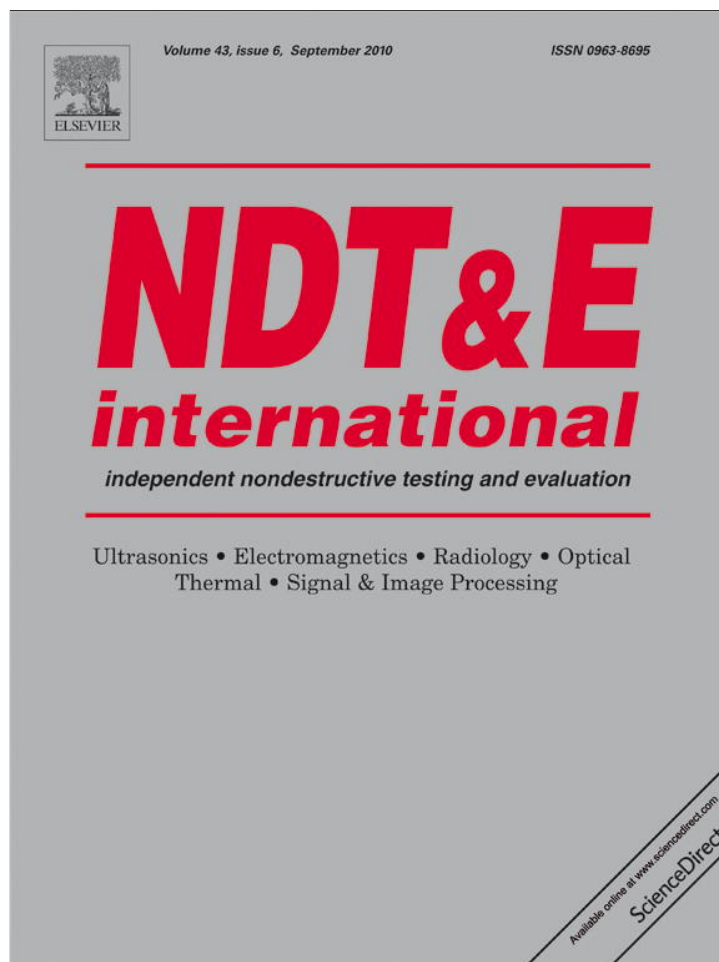


Provided for non-commercial research and education use.  
Not for reproduction, distribution or commercial use.



This article appeared in a journal published by Elsevier. The attached copy is furnished to the author for internal non-commercial research and education use, including for instruction at the authors institution and sharing with colleagues.

Other uses, including reproduction and distribution, or selling or licensing copies, or posting to personal, institutional or third party websites are prohibited.

In most cases authors are permitted to post their version of the article (e.g. in Word or Tex form) to their personal website or institutional repository. Authors requiring further information regarding Elsevier's archiving and manuscript policies are encouraged to visit:

<http://www.elsevier.com/copyright>



Contents lists available at ScienceDirect

NDT&amp;E International

journal homepage: [www.elsevier.com/locate/ndteint](http://www.elsevier.com/locate/ndteint)

## Development of auto defect classification system on porosity powder metallurgy products

Kuang-Chao Fan<sup>a,\*</sup>, Shou-Hang Chen<sup>a</sup>, Jhih-Yuan Chen<sup>a</sup>, Wei-Bor Liao<sup>b</sup>

<sup>a</sup> Department of Mechanical Engineering, National Taiwan University, Taipei, Taiwan, ROC

<sup>b</sup> Lenco Enterprise Co Ltd

### ARTICLE INFO

#### Article history:

Received 11 June 2009

Received in revised form

6 January 2010

Accepted 16 April 2010

Available online 4 May 2010

#### Keywords:

Automatic optical inspection

Powder metallurgy

Auto defect classification

Image processing

### ABSTRACT

Automatic optical inspection (AOI) has been applied to many manufacturing fields for defect inspection of mass production parts, such as PCB and TFT-LCD, but it has never been applied to the production line of porous powder metallurgy. By its nature, the powder-formed part has inherent non-uniform porosity pattern on the metal substrate. The defect's images are not easily separated from the substrate surface using the conventional binarization technique. This study develops a new image processing methodology and employs optical system design to build up an on-line surface defect inspection system for powder metallurgy parts. An analysis algorithm is also developed for the auto defect classification technique. It removes the noise signals from the porous image, detects the object edge and uses the hybrid-based method to sort out defects on the surface, such as crevice, scratch, broken corner and dent. Experimental tests show the maximum miss rate can be controlled to less than 5.65%.

© 2010 Elsevier Ltd. All rights reserved.

### 1. Introduction

In recent years, automated optical inspection (AOI) technology has been widely used in many industries for defect inspection and classification, such as PCB, TFT-LCD, etc. The AOI system scans the object images into the system and detects defects directly. In the past, the most popular application of AOI system is in the PCB industry [1]. Recently, this technique has been extended to TFT-LCD, IC, solar cell, and many other industries to replace labor-intensive manual inspection jobs [2]. There are numerous methods and mathematical algorithms in the area of AOI technology nowadays. Moganti et al. divided processing methods into three main types: reference-based, rule-based and hybrid-based [1]. According to Sanz and Jain [3], the defect inspection of PCB is mostly known by the referential-based method. The captured image is compared with a non-defect reference image that stores in the data base to detect a designated region of inspection (ROI). The image comparison algorithms used simple XOR logic operator to detect the defects. Akiyarnai et al. [4] developed the PCB defect detection method by referential template matching. The templates were compared with the inspected image to detect the large defects in the first place. They then used a logical AND operation for all sizes of defects to extract defect image. Huang et al. [5] developed an automated visual inspection system for detecting and classifying defects of a micro-

drill. The detection algorithm was based on the geometric relationship of the edge points in the ROI. The reference-based method needs alignment mark and precision moving mechanism to provide a stable image location for matching the pattern. The rule-based method needs to designate the object pattern and the ROI of image. It is difficult to change to the different sizes. The hybrid-based method combines the merits of the reference-based and the rule-based methods to compensate for the shortcomings of each method. Chang et al. [6] developed a hybrid-based method to detect the defects of the PCB in the transporting process. In the first stage, they retrieved and segmented the image with defects in the data base. Then, they compared the image with data base to recognize the defects. A variety of AOI systems have been applied extensively to IC [7–9], PCB [10,11], machine tools [12,13] and gas pipelines [14]. It is noted that all the above methods for defect inspection are based on a very clean template or ruled geometry. If there are already non-uniform noises on the template, it is difficult to identify the defects.

The image processing algorithm is a key to the AOI systems. There are many basic theories, such as auto threshold selection [15], edge detection [16–18], noise reduction [19], mask convolution, etc. It is generally called image pre-processing, which can be used to remove unwanted noises and enhance some important image features for further image processing.

Powder metallurgy uses the sintering process for manufacturing various parts in batches. After sintering in a controlled atmosphere at high temperature, the metal powder forms a solid piece. Such a process results in inevitable residual porosity on the surface. This kind of porosity is not a defect but a natural form

\* Corresponding author. Tel.: +886 2 2362 0032; fax: +886 2 2364 1186.  
E-mail address: fan@ntu.edu.tw (K.-C. Fan).

of such kind of product. This random porous pattern will, however, increase the difficulty in defect inspection by human eyes or AOI machine. To all powder metallurgy manufacturers, the trend becomes the need of small quantity and diverse products, namely the batch process. The defect inspection method of powder metallurgy products still relies on human eyes at present. It is not only subject to human errors but also consumes tremendous manpower and time. Therefore, to develop an AOI technology with cost-effective and high reliability of defect detection becomes necessary in modern powder metallurgy manufacture. There are rare AOI machines applied to the powder metallurgy product inspection. Lung and Fan [20] presented a preliminary AOI system for powder metallurgy products. However, the missing rate was still higher than expected.

The aim of this work is it attempts to develop an AOI system for powder metallurgy parts in order to replace manpower inspection, meanwhile, increase the production efficiency and decrease the miss detection rate resulting from human factor. An optical image system is integrated into a conveyer system to build up an auto defect classification (ADC) system on the production line. In the consideration of inspection method, due to the porosity surface of the powder metallurgy products, the image quality is not stable. Besides, the shapes of the product are variable from batch to batch. A fixed template can only deal with a particular shape. This research, therefore, proposes a hybrid-based method to identify and classify the defects. The influence of the porous surface can be eliminated first by the proposed double edge detection method for further defect identification and classification processes. The full field image of the part on the conveyor can be automatically captured with the aid of a limit switch. Therefore, high precision alignment mechanism and high resolution CCD camera are not necessary. It is aimed to provide a cost-effective solution to powder metallurgy industry.

## 2. Experimental set-up

For the purpose of real-time inspection, the image capturing system requires a suitable shutter speed, which is triggered by an optical limit switch, in order to acquire a clear image of the moving object. The moving speed of the object is about 120 mm/s. The shutter speed is about 2.5 ms. The CCD has  $764 \times 582$  pixels with 8-bit gray levels, and the resolution is around  $40 \mu\text{m}/\text{pixel}$ . A telecentric lens is mounted onto the CCD to provide consist dimension free from the height change. The focal length of the lens is 55 mm and the maximum depth of field is about 5 mm.

Lighting technique is crucial to the AOI system, especially when measuring the sizes or extracting the features. Fig. 1 shows

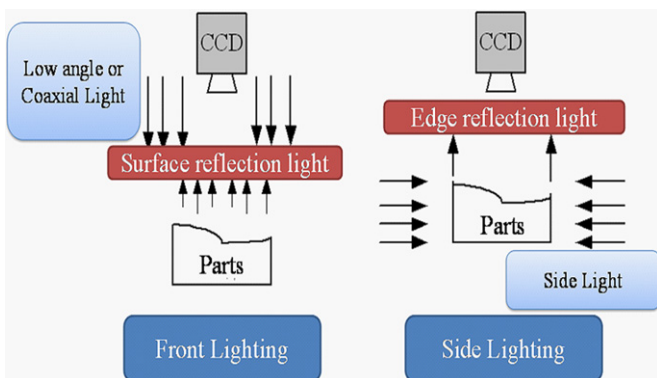


Fig. 1. Two lighting methods.

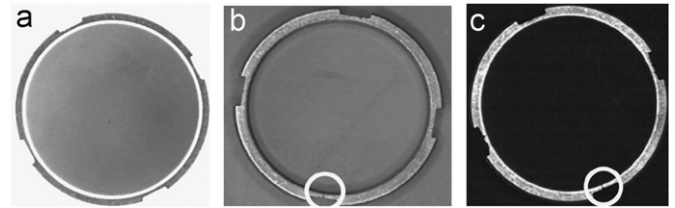


Fig. 2. The images illuminated by (a) side light, (b) low-angle light and (c) coaxial light.

two different lighting types, namely the front lighting and the side lighting. For different materials, we have to choose proper illuminations to highlight the defects image on the object surface. For the porous powder metallurgy part, the defects on the surface cannot be clearly seen when using the side lighting, such as the small scratch, as shown in Fig. 2a. There are two types of front lightings: low-angle lighting and coaxial lighting. Fig. 2b shows the image illuminated by low-angle lighting. Although it can suppress the porous feature, it also blurs the small defects, such as a scratch. This result will make the software inspection more difficult. So, the coaxial lighting has to be chosen and the captured image is shown in Fig. 2c. The defects can be seen conspicuously even if the scratch is small. Although the porous features also appear, we can use the image processing technique to remove them.

Fig. 3 shows the experimental set-up. The parts are pushed to the conveyor in sequence by a vibratory feeder. The photoelectric sensor triggers TTL signals to the camera while the part moves to the ROI. The AOI system captures the image, and then analyzes it and judges whether the part is good. If the part is defective, the air cylinder will push it away to a side guide way. Both sides of the part are to be inspected. The qualified part is slid to the next conveyor via a turn-over device. This turn-over device observes the law of gravity so that the part can be turned upside down while it slides down along the S-like sloped guide way due to initial momentum and self-weight. This is a powerless device. Fig. 4 shows the flow chart of the developed AOI system operation.

## 3. Powder metallurgy defects

The need of an AOI system is not only to be able to identify the defects on the parts but also to classify the defect type for statistical process control. Conventional reference-base method cannot be applied to the porous surface because the porosity pattern is different to each part. The porosity is not a defect but the nature of this kind of surface. In our works, we present the hybrid-based method that is to create rules for the reference image, rather than just matching the image. After the learning process, a learning value is selected to find the defects.

### 3.1. Defects of the seal

Usually, the defects of the powder metallurgy product result from several factors that include feed, unscramble, transportation, sintering and finishing. In this work, we use seal rings pressed from stainless steel powders as our first testing samples, as shown in Fig. 5. The outer diameter is about 22 mm and the inner diameter is about 17.8 mm. The defects of a seal ring can be classified into four types as follows:

- (1) Crevice: When the parts are in sintering process, if the residual stress is released unevenly, it will produce a crevice

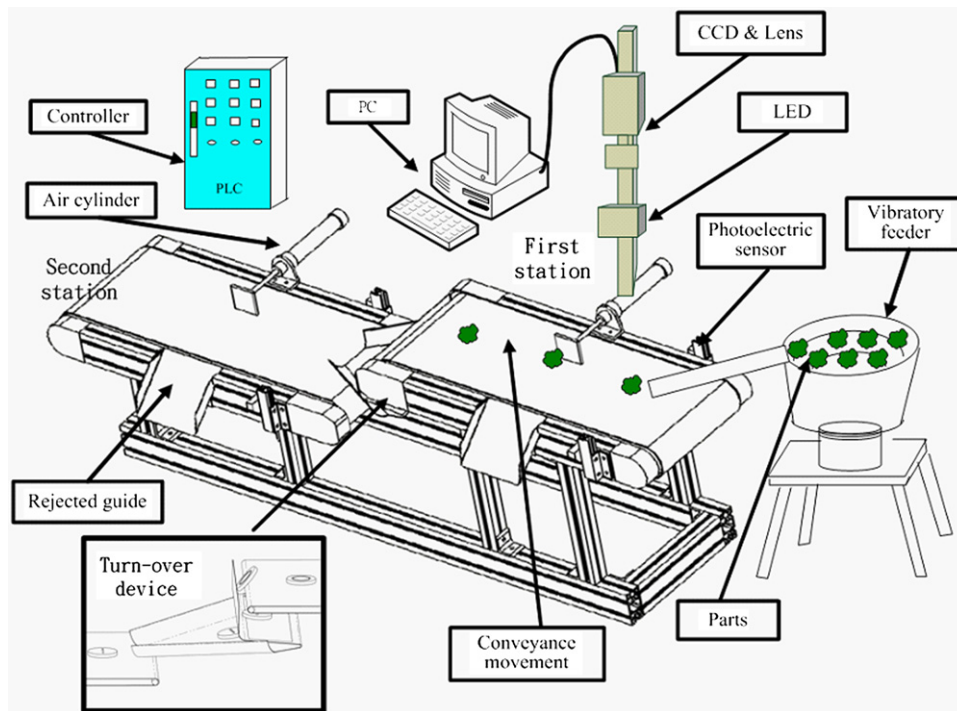


Fig. 3. System diagram of the AOI equipment.

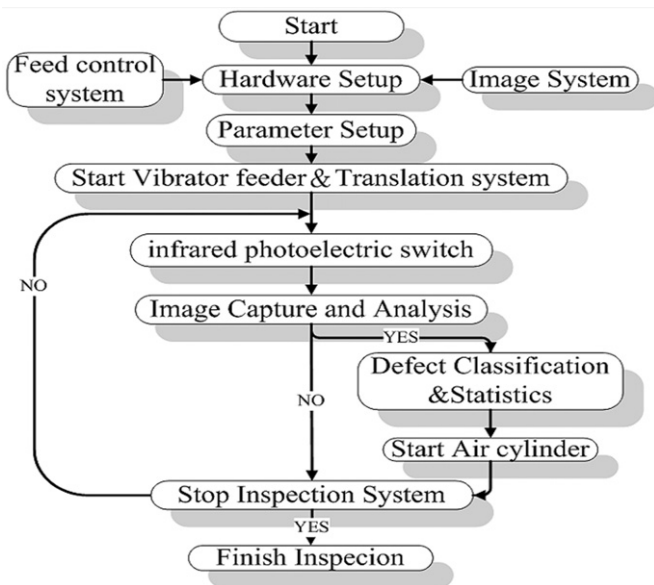


Fig. 4. Flow chart of the AOI system operation.

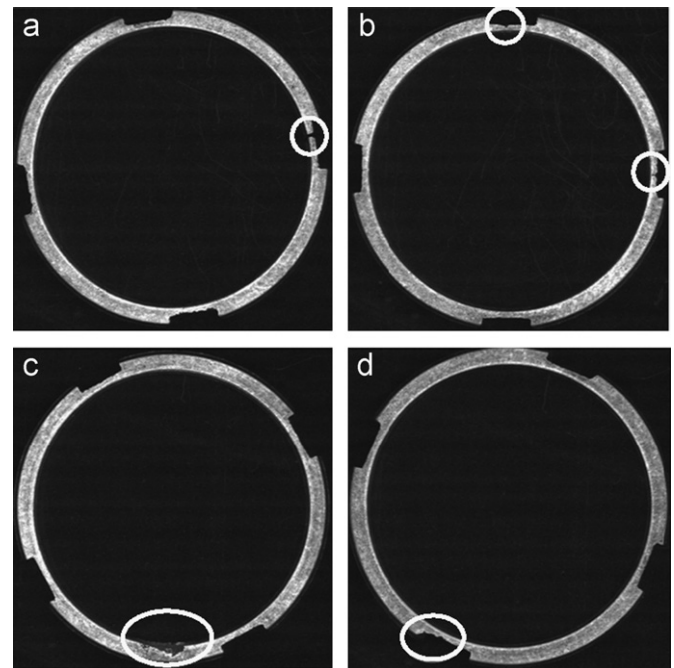


Fig. 5. Four defect types of the seal: (a) crevice, (b) scratch, (c) dent and (d) broken corner.

- defect on the surface or at the edge, as shown in Fig. 5a. This is defined as the breakage of the groove.
- (2) Scratch: It comes out from the abrasive mold or the scratch during part transportation and sintering, as shown in Fig. 5b. It usually happens on the groove region.
  - (3) Dent: This kind of defect is caused by foreign particles on the mold surface, part collision and adhesive congregation, as shown in Fig. 5c. It happens on the ring's outer or inner peripheral.
  - (4) Broken corner: This is due to non-uniform powder filled in the mold or wrong powder size selection, as shown in Fig. 5d. It happens on the groove corner.

### 3.2. Auto defect classification

Most manufacturers need to know not only the number of defects on the production line but also the defect types in order to carry out the statistical process control. Auto defect classification technology (ADC) is, therefore, a necessary tool to meet this requirement. After analyzing the defect data, process parameters can be tuned properly in order to improve the quality.

Rare researches on the ADC technology have been done on powder metallurgy production, despite the growing demand on the AOI market [20]. It is because varied defects need different solutions and the computation time for feature extraction may decrease the throughput rate. In this work, a fast feature extraction algorithm is proposed to separate each feature of defect. Compared to the whole image size, the quantity of feature information is relatively small. After the feature extraction, pixels to be computed are only those feature parts. A substantial computation time can be saved.

#### 4. Defect inspection and classification

In the general image processing technique, the auto threshold method is usually used to separate the object from the background when the background is clean. Such a technique, however, cannot be simply applied to the porous surface because although the porosity creates unwanted noise on the image it is not a defect, as shown in Fig. 6a. When porous particles are widely distributed over the object surface, an auto threshold method, such as the Otsu's algorithm [15], will still remain as noise on the background, as shown in Fig. 6b. The gray level distribution of a typical porous surface, such as a seal ring, is plotted in Fig. 6c. It is seen that except the black background that dominates the gray levels around 20, the remaining pixels contain two groups of gray levels: the small group around 50 representing the edge and defect points and the large group representing the porous points. Therefore, in order to extract the edge features and defect features, a new algorithm of the auto threshold method by double edge detection is developed in this paper.

##### 4.1. Double edge detection method

In this method, the Canny operator of edge detection [16] is first used to find out the location of pixels which include the object edge, defects, and some noisy profiles caused by the porous surface, as shown in Fig. 7a. As shown in the enlarged chart, each porous profile forms a small feature with higher gray level than

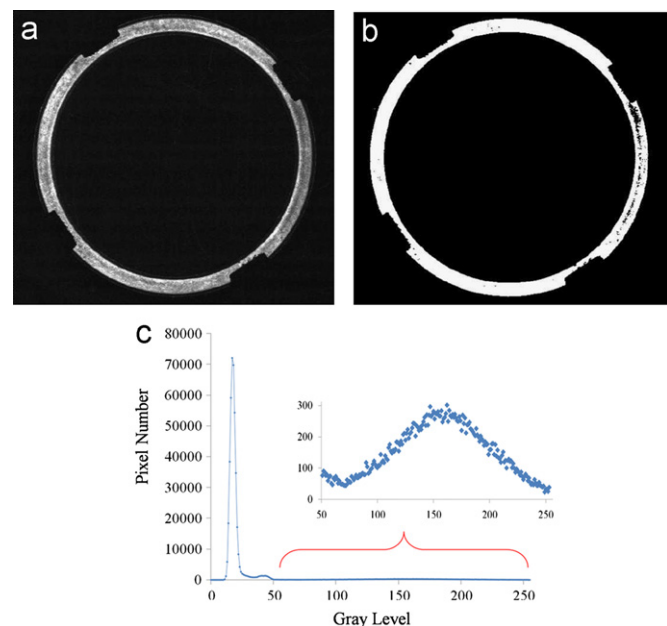


Fig. 6. Image processing: (a) original image, (b) after Otsu's algorithm, (c) gray level distribution of original image.

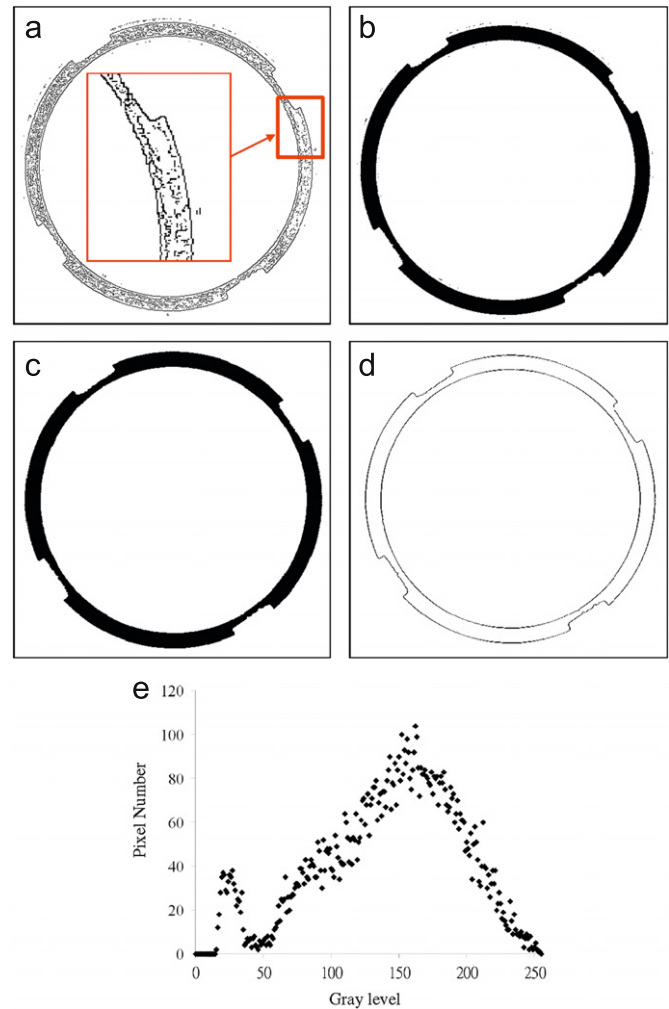


Fig. 7. Image pre-processing, (a) after edge detection, (b) after binarization and gray level inverse, (c) after noise removal, (d) after edge detection, (e) gray level distribution of (a).

the defected points and edge points. The gray levels of all pixels out of the background are then collected and sorted in an increasing order of  $G_i[N_i]$ , where  $N_i$  is the number of pixels corresponding to  $G_i$ . The distribution of  $G_i[N_i]$  is shown in Fig. 7e. The group under gray level 50 contains the edge and defect points, while those above are the porous signals. A clear separation point can be seen. Therefore, the best threshold value is obtained by the following equation:

$$G_{\text{best}} = G[N \times \delta_{\text{ratio}}] \quad (1)$$

where  $\delta_{\text{ratio}}$  is a constant, which is chosen as 0.07 from experiments and  $N$  is the total number of pixels (sum of  $N_i$ ). After this binarization process, the gray levels are inverted so that the porous effect is eliminated from the surface, as shown in Fig. 7b. Again, in order to remove the surrounding noise, the eight-connectivity method is employed, as shown in Fig. 7c. The edge detection method is then applied again to acquire the edge profile and to calculate the feature information, as shown in Fig. 7d. The novelty of the presented method is that using double edge detection technique the local porous profiles can be totally removed out from the edge and the defect profiles. In order to demonstrate the effectiveness of this double edge detection technique to the porous products, two more tests are taken on two other samples, i.e., a square porous pad and a small porous

gear. As shown in Fig. 8, even though these two objects have worse porous surfaces they can be easily cleaned rapidly.

#### 4.2. Feature extraction

After the double edge detection process, the contour of the inspected seal ring is divided into four segments: (1) the ring's inner contour segment, (2) the ring's outer contour segment, (3) the groove bottom segment and (4) the groove side segment, as shown in Fig. 9. Because segment 1 is an independent inner contour, it can be easily singled out. The actual outer contour of this object contains segments 2, 3 and 4. In order to extract the feature of the ring's outer contour, the Hough transform method [21] is applied. This is a point-line mapping operation that converts the Cartesian coordinate ( $x-y$  space) to a polar coordinate ( $\theta-\rho$  space) through the following formula:

$$\rho = x \cos \theta + y \sin \theta \quad (2)$$

where  $\rho \in R$  is the distance from the origin to the line, and  $\theta \in [0, 2\pi]$  is the angle between the line and the horizontal axis. Segments 2, 3 and 4 are thus converted to three connected lines in different slopes, as shown in Fig. 10. The ordinate represents the distance of each feature from the center of the ring.

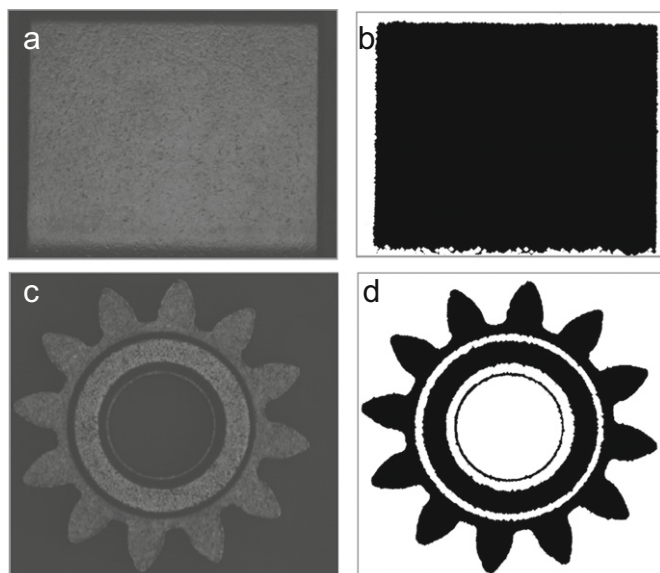


Fig. 8. Two test objects and results: (a) original square pad image and (b) its processed result; (c) original gear sample image and (d) its processed result.

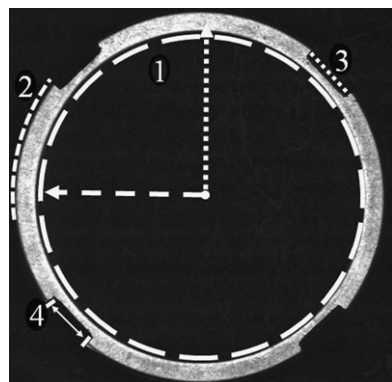


Fig. 9. Four segments of the seal ring.

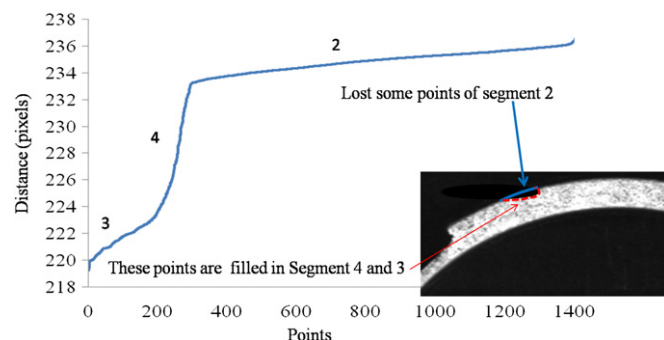


Fig. 10. The distance between the point of the outer contour and the center of the seal ring; the thick line represents no defect and the thin line represents a dent defect.

It has to be pointed out here that the dent defect would more or less affect the corresponding segment line shape. When a minor dent appears on the ring's outer contour, for instance, as shown in the enlarged image in the new Fig. 10, it will be treated as a small groove with longer distance from the origin. Then, segment 2 will be shortened due to reducing points and segment 4 will be lengthened with more points and, accordingly, its slope is reduced a little, as given by the red lines. Conversely, if the dent is too big, the calculated center of origin and radius will be significantly deviated from the nominal data. This part will be automatically rejected by the program without going to the following defect detection process. This decision applies to the big dent happening on the inner contour and the groove contour.

The Hough transform has the advantage of robustness against noise. However, it also has some limitations [22]. In this case, Lines 2 and 3 are relatively short compared to Line 4. In practice, it is hard to divide three segments simultaneously. Therefore, three times of Hough transform processes are operated to separate these three segments in sequence. The first step can extract the ring's outer contour segment (Fig. 11a), the second step is to gain the groove bottom segment (Fig. 11b) and the third step can obtain the groove side segment (Fig. 11c). At the junction between two segments, it is hard to differentiate which portion those points belong. A few junction points are deliberately removed in order to identify each segment. After removing some corner points, the final result is shown in Fig. 11d.

#### 4.3. The defect classification rules

In this work, four kinds of defect are to be inspected for the seal ring. These are:

- (1) Crevice defect inspection: After pre-processing, the image features can be used to directly detect the crevice defect. A non-defect image has two circular contours, namely the inner contour and the outer contour, as shown in Fig. 12a. When only one crevice happens on the seal ring, these two contours will be connected and become only one contour, as shown in Fig. 12b. If there are two crevices, it will result in two contours and all are not circular. Consequently, more crevices generate more non-circular contours. By this phenomenon, the definition of crevice defect is determined by the number of contours and the roundness of the inner contour.
- (2) Dent defect inspection: After image binarization, the object can be separated from the background. The outside and inside radii are calculated and the corresponding circular contours are extracted. Taking out these two circular portions by the filtering process, it will appear four remaining groups representing the groove contours, as shown in Fig. 13. Comparing the remaining

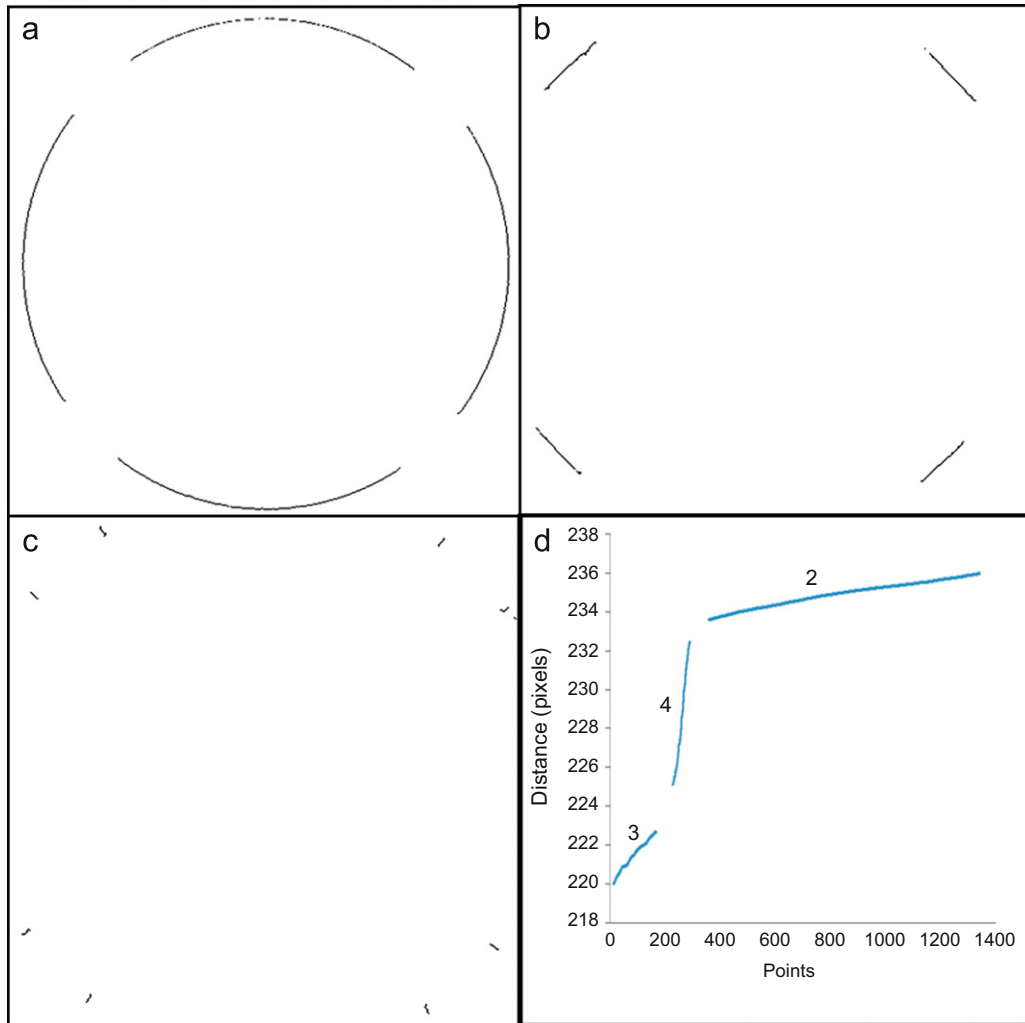


Fig. 11. Feature extraction of outer contour: (a) segment 2, (b) segment 4, (c) segment 3, (d) Hough transform result.

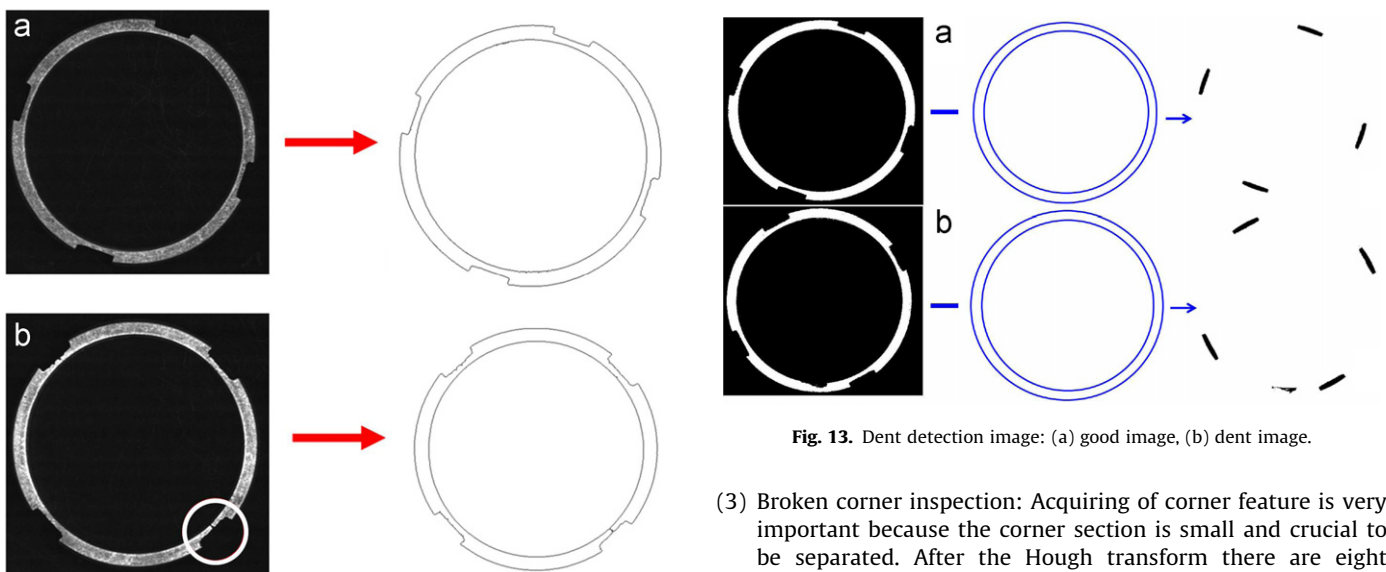


Fig. 12. Crevice detection: (a) good image, (b) defect image.

Fig. 13. Dent detection image: (a) good image, (b) dent image.

groups with a reference image, the dent portion can be identified by the reference-based method. Therefore, the definition of dent defect is the number of remaining pixels.

(3) Broken corner inspection: Acquiring of corner feature is very important because the corner section is small and crucial to be separated. After the Hough transform there are eight segments of no. 3 representing the groove sides, as given in Figs. 11c and 14. The distance of the paired-sides represents the groove width. If the calculated width  $d$  in Fig. 14b is larger than the learning value, the broken corner is identified. Therefore, the definition of the broken corner defect is the distance of two no. 3 segments of the corresponding groove.

(4) Scratch defect inspection: This kind of defect is hard to be detected by manpower because it has to be observed from different angles. From experience, the scratch defect always happens at the edge and the surface of the groove. Fig. 15a shows a non-defect image, where segment no. 4 is approximated to a straight line. However, when there is a scratch defect, the straight lines would become indented or generate a “V” shape, as shown in Fig. 15b. We can fit segment no. 4 by a straight line and calculate its straightness. If the straightness error is out of the learning value, the scratch is determined. Therefore, the definition of scratch defect is the maximum residual value of the straightness with contour points.

From the above logical analysis, the learning parameter corresponding to each type of defect can be summarized in Table 1.

#### 4.4. The inspection process

According to the above-mentioned analysis of defect classification, a software program for dimension and defect inspections is developed with C++ language around a PC with 2.4 GHz CPU and 2 GB RAM. This program has been successfully applied in a circular shape analysis with a sub-pixel technique [23]. The sequence of defect inspection is illustrated in the flow chart of

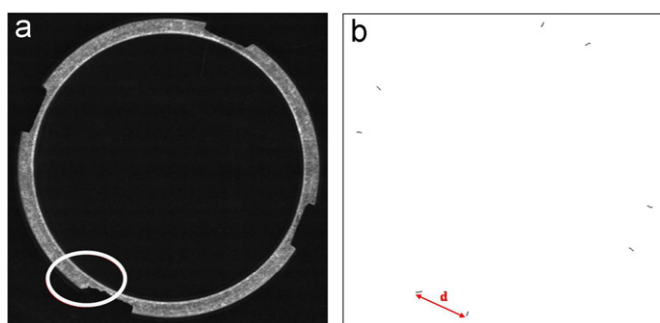


Fig. 14. Broken corner detection: (a) original image, (b) identify corner width.

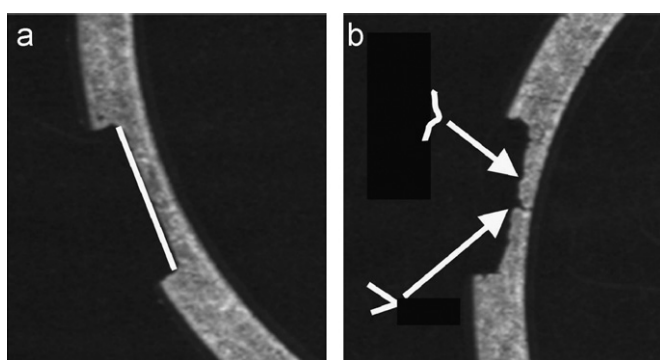


Fig. 15. A detailed image of scratch defect: (a) straight line, (b) indented line.

Table 1  
Definitions for defect classification.

Defect	Crevice	Dent	Scratch	Broken corner
Learning parameter	The number of contour, the shape of contour	The number of remaining pixels	Groove straightness	Groove width

Fig. 16. Right after the feature extraction process, as indicated in Section 4.2, the dent defect can be sorted out by the calculated radii and the remaining pixels, and the crevice can be identified by the contour number of the remaining pixels. Then, using the straightness of the groove contour the scratch is classified, and finally with the dimension of groove width the broken corner is identified. All defect parts will be automatically pushed out from the conveyor by an air ejector. The processing time for one image is about 0.15 s, which is fast enough to meet the feed rate of the parts.

## 5. Experimental results

### 5.1. Repeatability test

The repeatability test is carried out on a single seal ring with ten times of inspection. Calculated parameters are the outer radius, the inner radius and the groove width. Results are listed in Table 2. The maximum standard deviation is less than 0.3 pixels. The AOI system has been calibrated by a standard template and one pixel corresponds to about 50 μm. This repeatability result is satisfied by the factory people.

### 5.2. Training of learning values

The learning parameter for each defect type has been given in Table 1. These parameters have to be trained to get the proper corresponding learning values. Initially, seventy parts of the seal ring are selected and inspected by a skillful technician in the factory. There are three pieces of dent, twelve pieces of broken corner, twenty-five pieces of scratch defect and twenty-nine non-defect parts. Fig. 17 shows the process results of dent defect learning and the learning value of remaining pixels are found to be about 61. Fig. 18 shows the process results of broken corner learning and the critical value of groove width is about 79. Fig. 19 shows the process results of scratch learning and the straightness value is about 2.7. Unfortunately, this batch of samples does not have crevice defect, there is no experimental result of this type. The crevice defect, however, is very clear in the image. It is not difficult to be sorted out by the judgment of Section 4.3 (1).

### 5.3. Tuning of learning values

The learning values obtained from the above comparison with human eyes may not be the best ones as, seen from Figs. 17–19, there is always a bandwidth, or the gap, of each proper learning value between the good samples and the faulty samples. In this experiment, a repeatability test is carried out in order to find out the best learning values. The maximum allowable learning value of each defect is chosen from Figs. 17–19. One hundred times of image from random samples are captured. The inspected results are listed in Table 3. The standard deviation of dent, scratch and broken corner defect are 2.41, 0.28 and 0.21, respectively. Comparing the deviation value with the range of the gap, the learning values of dent, scratch and broken corner are tuned to be 60, 3.5 and 78 eventually.

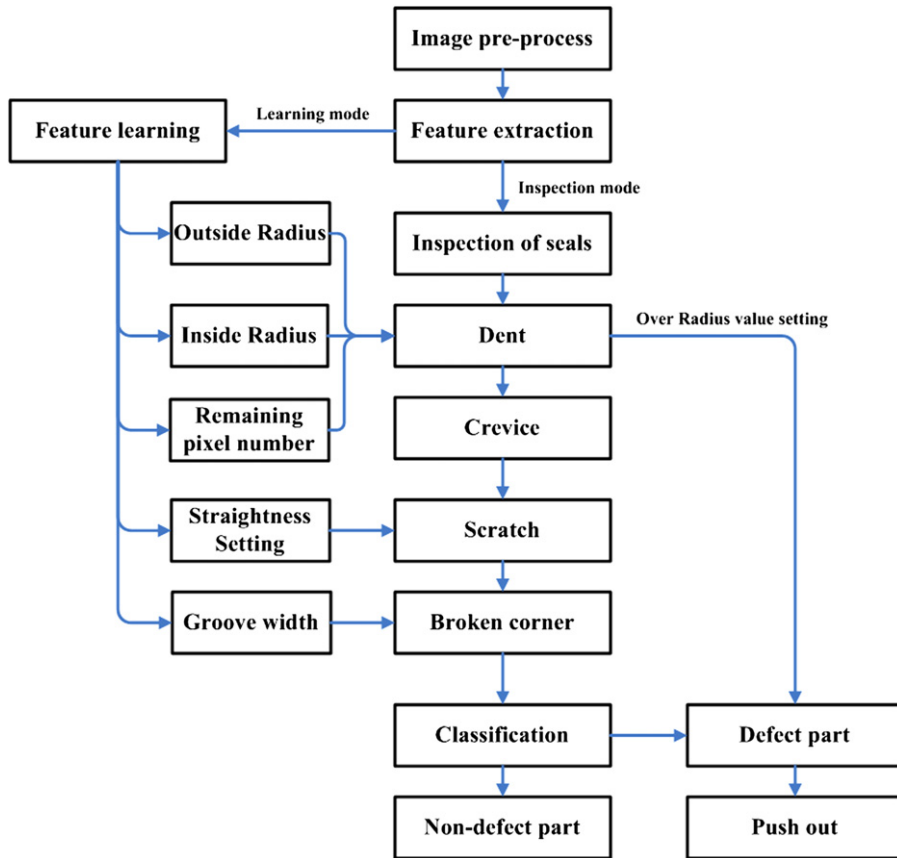


Fig. 16. Flow chart of inspection procedure.

Table 2  
Repeatability test (unit: pixel).

No.	Outer radius	Inner radius	Groove width
1	230.4	198.4	68.5
2	230.3	198.4	68.6
3	230.8	198.4	68.2
4	230.5	198.5	68.3
5	230.7	198.5	68.3
6	230.5	198.5	67.8
7	230.8	198.4	68.0
8	230.4	198.4	67.9
9	230.9	198.4	67.9
10	230.4	198.4	68.3
Avg.	230.57	198.43	68.18
Std.	0.198	0.025	0.263

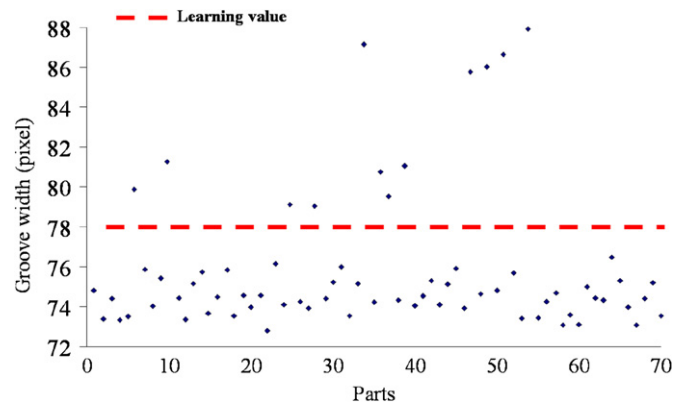


Fig. 18. The process results of broken corner defect.

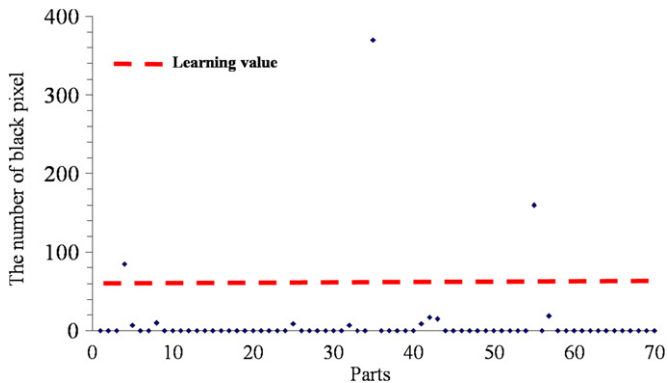


Fig. 17. The process results of dent defect inspection.

#### 5.4. Batch repeated inspection

Finally, a long term batch test is implemented along the production line in order to validate the accuracy of the developed AOI system. With the help of factory technicians, 100 non-defect parts and 150 defect parts are selected. One hundred times of repeated tests to all 250 parts have been done by the system shown in Fig. 3. The results are listed in Table 4. The miss rates of non-defect part, scratch defect and broken corner defect are 5.65%, 4.38% and 0.4%, respectively. No miss rate happens to the dent and crevice. It is evident that the proposed AOI system for defect inspection of porous part can assure fast and reliable results. Although the miss rate can be improved by tuning the user defined learning values, it will pass more defect parts. This is not what the factory wants.

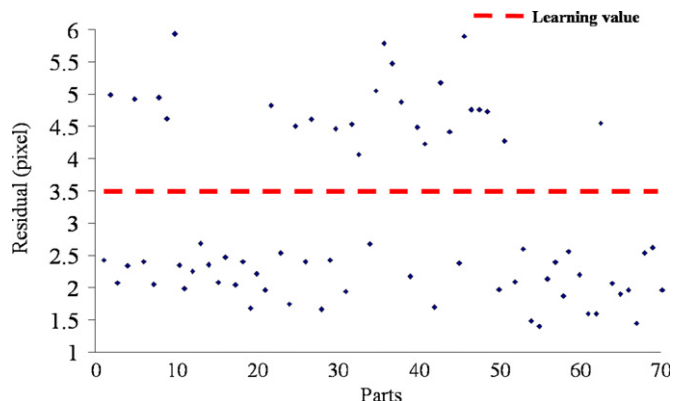


Fig. 19. The process results of scratch defect.

Table 3  
Repeatability test results and the learning values.

Defect	Dent defect	Scratch	Broken corner
Max/Min value	25/19	3.05/2.23	76.83/76.28
Standard deviation	2.41	0.28	0.21
Learning value	60	3.5	78

Table 4  
Long term test results.

Defect type	Total number	Non-defect	Dent	Crevice	Scratch	Broken corner	Miss rate %
Non-defect	100	94.35			5.65		5.65
Dent	10		10				0
Crevice	60			60			0
Scratch	60	2.63			57.37		4.38
Broken corner	20	0.08				19.02	0.4

6. Conclusions

This study has successfully developed an automatic optical inspection system for detecting the defects of porous powder metallurgy products. Powder metallurgy product has a serious porous surface that does not have a stable binarization image by the traditional auto threshold method. A technique of double edge detection method is thus proposed to remove the non-uniform porosity effect. The selected samples for test are of a circular shape. Using the Hough transform technique, all contour features can be extracted. Applying the proposed hybrid-based method, four types of defect, namely dent, crevice, scratch and broken corner, can be classified by the selection of best learning values. Experimental results show the repeatability is high and the miss rate is low with batch inspection on the factory side. The developed system is suitable for on-line automatic defect inspection of powder metallurgy parts of circular shapes.

It is known that most surface defects are similar in different products, such as IC, PCB, FPD, mechanical part, etc. Although the developed defect inspect method is suitable for products with circular shape, with proper analytical algorithm it is not difficult

to deal with other kinds of product. The novelties of this system are: (1) the separation of required object features from noisy substrate by the proposed double edge detection method, (2) the classification of defect type by the proposed hybrid-based method, and (3) the robustness for long term operation. In fact, this system has been operating in the factory for more than six months already without problem. It helps replace tedious and eye-damaging manual work, and contribute to the investment return in a short period. Future works will cope with parts of different shapes by studying more hybrid-based analytical algorithm.

Acknowledgements

The authors gratefully acknowledge the support of Lenco Enterprise Co. Ltd for this work.

References

- [1] Moganti M, Ercal F, Dagli CH, Tsunekawa S. Automatic PCB inspection algorithms: a survey. *Computer Vision and Image Understanding* 1996;63(2):287–313.
- [2] Fan KC, Hsu C. Strategic planning of developing automatic optical inspection (AOI) technologies in Taiwan. *Journal of Physics Conference Series* 2005;13:394–7.
- [3] Sanz JLC, Jain AK. Machine-vision techniques for inspection of printed wiring board and thick-film circuits. *Journal of Optical Society* 1986: 1465–82.
- [4] Akiyama Y, Hara N, Karasaki K. Automatic inspection system for printed circuit boards. *IEEE Transactions on Pattern Analysis and Machine Intelligence (PAMI)* 1983;5(6):623–30.
- [5] Huang CK, Liao CW, Huang AP, Tarng YS. An automatic optical inspection of drill point defects for micro-drilling. *International Journal of Advanced Manufacturing Technology* 2008;37:1133–45.
- [6] Chang PC, Chen LY, Fan CY. A case-based evolutionary model for defect classification of printed circuit board images. *Journal of Intelligent Manufacturing* 2008;19(2):203–14.
- [7] Maeda S, Kubota H, Makihira H, Ninomiya T, Nakagawa Y, Taniguchi Y. Automated visual inspection for LSI wafer multilayer patterns by cascade pattern matching algorithm. *Systems and Computers in Japan* 1990;21(12):65–77.
- [8] Scaman ME, Economikos L. Computer vision for automatic inspection of complex metal patterns on multichip modules (MCM-D). *IEEE Transactions on Components, Packaging, and Manufacturing Technology, Part B: Advanced Packaging* 1995;18(4):675–84.
- [9] Shapiro A. Automatic classification of wafer defects: Status and industry needs. In: *Proceedings of the IEEE/CPMT international electronics manufacturing technology (IEMT) symposium, 1996*; p. 117–22.
- [10] Hara Y, Akiyama N, Karasaki K. Automatic inspection system for printed circuit boards. *IEEE Transactions on Pattern Analysis and Machine Intelligence (PAMI)* 1983;5(6):623–30.
- [11] Nagaswami VR, Grimeault S, Dover RJ. Application of segmented auto threshold (SAT) for 0.5 μm and 0.35 μm logic interconnect layers. *IEEE/SEMI Advanced Semiconductor Manufacturing Conference and Workshop, 1997*.
- [12] Fernandez C, Fernandez S., Campoy P., Aracil R. On-line texture analysis for flat products inspection. *Neural nets implementation*. In: *Proceedings of IECON 1994*; p. 867–72.
- [13] Marino P, Dominguez MA, Alonso M. Machine-vision based detection for sheet metal industries. In: *Proceedings of IECON, San Jose, CA, USA, Institute of Electrical and Electronics Engineers Computer Society, 1999*; p. 1330–5.
- [14] Shafeek HI, Gadelmawla ES, Abdel-Shafy AA, Elewa IM. Automatic inspection of gas pipeline welding defects using an expert vision system. *NDT and E International* 2004;37(4):301–7.
- [15] Otsu N. A threshold selection method from gray-level histograms. *IEEE Transactions on Systems, Man and Cybernetics (SMC)* 1979;9(1):62–6.
- [16] Canny J. Computational approach to edge detection. *IEEE Transactions on Pattern Analysis and Machine Intelligence (PAMI)* 1986;8(6):679–98.
- [17] Elder JH, Zucker SW. Local scale control for edge detection and blur estimation. *IEEE Transactions on Pattern Analysis and Machine Intelligence* 1998;20(7):699–716.
- [18] Marr D, Poggio T. Theory of edge detection. *Proceedings of Royal Society, London* 1980;B207:187–217.
- [19] Wu WY, Wang MJJ, Liu CM. Performance evaluation of some noise reduction methods. *CVGIP: Graph Models Image Process* 1992;54(2):134–46.

- [20] Lung CY, Fan KC Automatic optical inspection on porosity powder metallurgy products. Proceedings of the second international symposium on instrumentation science and technology, Hefei, China, Harbin Institute of Technology, 2002: p. 142–7.
- [21] Deans SR. Hough transform from the radon transform. *IEEE Transactions on Pattern Analysis and Machine Intelligence* 1981;3(2):185–8.
- [22] Han QL, Zhu M, Yao ZJ. A segment detection method based on improved Hough transform. Proceedings 20th Congress of the International Commission for Optics 2005:272.
- [23] Fan KC, Chen JY, Wang CH, Pan WC. Precision in-situ volume measurement of micro droplet. *Journal of Optics A: Pure and Applied Optics* 2009; 11(1):1–8.